Efficient molecular dynamics in Coulomb systems with two-dimensional periodicity: Application to polyelectrolyte brushes

Takamichi Terao
Department of Applied Physics, Hokkaido University, Sapporo 060-8628, Japan
(Received 16 May 2002; published 30 October 2002)

We study polyelectrolyte brushes in an electrolyte solution by molecular dynamics simulations. The efficient calculation method to treat the Coulomb systems with two-dimensional periodicity is presented, employing the particle-cell acceleration technique and the Lekner summation method. The structural formation of polyelectrolyte brushes and the electrostatic screening effect with monovalent salts are clarified numerically. The calculated results show the dependence of the structural formation in polyelectrolyte brushes on the grafting density and the concentration of added salts. The calculated results show the dependence on the grafting density and the concentration of added salts in the structural formation of polyelectrolyte brushes.

DOI: 10.1103/PhysRevE.66.046707 PACS number(s): 02.70.Ns, 82.70.−y, 82.35.Rs, 61.20.Ja

I. INTRODUCTION

Charged soft matters (i.e., charged colloids, charged gels, and polyelectrolytes) have attract much attention, where many-body Coulomb interaction plays a crucial role [1–10]. These are of importance as various industrial materials and biological systems. Recently, interesting physical phenomena have been pointed out and studied theoretically and experimentally, such as *charge inversion* [8,9], *like-charged attraction* [7], and *like-charged adsorption* [10]. These studies have clarified that the strength of Coulomb couplings Γ ($\Gamma \equiv E_c/k_BT$) is an essential parameter in these phenomena, where E_c, k_B, and T are the characteristic energy of Coulomb interaction, the Boltzmann constant, and the temperature of the system, respectively.

In general, computer simulations with an N-body Coulomb system are very time consuming, and it is difficult to treat many particles by direct calculations such as the particle-particle summation. To solve this difficulty, several rapid calculation techniques have been developed in the study of molecular simulations, for example, the particle-particle particle-mesh method and the particle-mesh Ewald method [11]. However, these numerical methods consider the three-dimensional periodic systems and are not applicable to the system with low-dimensional periodicity [12], including surfaces and interfaces. Recently, soft materials under geometrical confinement have attracted much attention, and it is very interesting to treat these problems with efficient algorithms.

In this paper, we pay attention to *polyelectrolyte brushes* and clarify their physical properties. Polyelectrolyte brushes are polymer layers at a solid-liquid interface where charged polymer chains are anchored by one end on a surface, and they are interesting subjects with many unresolved problems [13–17]. It is well known that polymer (polyelectrolyte) brushes are useful materials, for example, to avoid the flocculation between colloidal particles and stabilize colloidal suspensions in solutions [18–20]. We perform molecular dynamics simulations of polyelectrolyte brushes in an electrolyte solution. The full Coulomb interaction is treated in the numerical calculations, and counterions as well as added salts are included explicitly. In general, this task is very time consuming in a brush geometry with partially periodic systems, where a straightforward application of Ewald sums is not possible. We introduce the *particle-cell technique* to accelerate the molecular dynamics simulations, which makes the computation much faster and enables us to treat large number of particles in the system. To study the screening effect by adding salt ions, it is necessary to study the system with a lot of charged particles, and our approach is suitable for this purpose.

This paper is organized as follows. In Sec. II, we describe the model of polyelectrolyte brushes in solution. In Sec. III, the numerical method we introduce in this study is explained. We also show the calculated results on polyelectrolyte brushes in solutions. Section IV gives the conclusions.

II. MODELS

In this section, we describe the model of polyelectrolyte brushes in an aqueous solution. The negatively charged polymer chains are anchored to the grafting surface by means of an uncharged end segment (Fig. 1). We treat the polyelectrolyte brush systems with M polyelectrolyte chains, containing L charged monomers per chain, and $M \times L$ monovalent counterions due to the electrostatic neutrality. The anchor segments form a square lattice with the grafting density ρ per unit area σ^2. The system size is taken to be L_{xy} in the x and y directions and L_z in the z direction, where the grafting density ρ is defined to be $\rho = M\sigma^2/L_{xy}^2$. The temperature of the system is given by $k_BT = 1.2\epsilon_{LJ}$ (ϵ_{LJ} is the unit of energy). We impose periodic boundary conditions in the x and y directions, and a hard-wall boundary condition in the z direction. The discrete structure of the solvent is neglected, and the solvent enters into the model via its dielectric constant ϵ, which reduces the Coulomb interaction.

The potential energy of the system has four contributions:

$$V = \sum_{i<j}\sum \{V_{repul}(r_{ij}) + V_{Coulomb}(r_{ij}) + V_{bond}(r_{ij})\} + \sum_{i=1}^{N} V_{wall}(\{z_i\}), \quad (1)$$

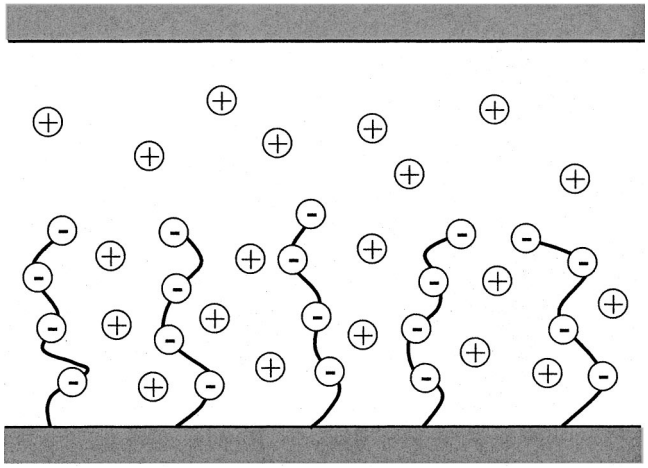

FIG. 1. The model of polyelectrolyte brushes in this study.

where r_{ij}, $V_{repul}(r_{ij})$, $V_{Coulomb}(r_{ij})$, $V_{bond}(r_{ij})$, and $V_{wall}(z_i)$ denote the distance between particles i and j, the excluded-volume interaction, the Coulomb interaction, the bond potential between neighboring polymer segments, and the repulsive interaction from the wall in the z direction, respectively. The excluded-volume interaction $V_{repul}(r_{ij})$ is given by

$$V_{repul}(r_{ij})=\begin{cases} 4\epsilon_{LJ}\left\{\left(\dfrac{\sigma}{r_{ij}}\right)^{12}-\left(\dfrac{\sigma}{r_{ij}}\right)^{6}+\dfrac{1}{4}\right\} & \text{for } r_{ij}\leqslant r_c \\ 0 \quad \text{for } r_{ij}>r_c, \end{cases} \tag{2}$$

where σ and r_c are the diameter of particles and the cutoff radius, respectively, and r_c is defined as $r_c\equiv 2^{1/6}\sigma$. In the following calculation, monomers, counterions, and added salt ions have the same diameter σ.

The Coulomb interaction in this system $V_{Coulomb}(r_{ij})$ is given by

$$V_{Coulomb}(r_{ij}) = \frac{e^2}{4\pi\epsilon\epsilon_0}\sum_{n_x=-\infty}^{\infty}\sum_{n_y=-\infty}^{\infty}\frac{q_i q_j}{|\mathbf{r}_{ij}+n_x L_{xy}\mathbf{e}_x+n_y L_{xy}\mathbf{e}_y|}, \tag{3}$$

where $\mathbf{e}_x$ and $\mathbf{e}_y$ are unit vectors in the x and y directions, respectively, and the indices n_x and n_y run over the periodic images of the simulation box. In Eq. (3), e, q_i, ϵ_0, and ϵ are the elementary charge, the charge of particle i in units of e, a dielectric constant of the vacuum, and the relative dielectric constant of the medium, respectively. The neighboring polymer segments i and j are coupled by the bonding potential $V_{bond}(r_{ij})$ as

$$V_{bond}(r_{ij})=\frac{1}{2}K_{bond}r_{ij}^2, \tag{4}$$

where K_{bond} is a constant. In addition, the hard-wall potential with the z direction, $V_{wall}(z_i)$, is given by

$$V_{wall}(z_i)=V_{repul}(z_i+\Delta z), \tag{5}$$

where z_i is the distance of the ith particle from the wall and Δz is defined as $\Delta z\equiv(2^{1/6}-1/2)\sigma$.

III. NUMERICAL RESULTS

We perform molecular dynamics simulations to study the structural formation of polyelectrolyte brushes in equilibrium. Treating the long-range Coulomb interaction in a quasi-two-dimensional system described by Eq. (3), we employ the Lekner summation technique, which shows great success in application to various problems such as colloidal suspensions and biomolecules [21–23]. Long-range interactions present a serious problem in molecular dynamics simulations as well as Monte Carlo simulations, because of the slow convergence of the sum over the repetitions of the central cell. In the Lekner summation technique, Coulomb summations are transformed to rapidly convergent ones via the Euler transformation and the Poisson-Jacobi identity.

In quasi-two-dimensional systems, the pair-potential $V(x,y;z)$ can be rewritten as

$$V(x,y;z)=\frac{q_i q_j e^2}{4\pi\epsilon}\Bigg[4\sum_{n=1}^{\infty}\sum_{k=-\infty}^{\infty}K_0(2\pi n\sqrt{(y+k)^2+z^2}) \times\cos(2\pi n x)-\ln\{\cosh(2\pi z) -\cos(2\pi y)\}+c_2\Bigg], \tag{6}$$

where $K_0(x)$ and c_2 are the modified Bessel function and the constant to be added, respectively [21]. Equation (6) can be also written as

$$V(x,y;z)=\frac{q_i q_j e^2}{4\pi\epsilon}\Bigg[4\sum_{n=1}^{\infty}\sum_{k=-\infty}^{\infty}K_0(2\pi n\sqrt{(x+k)^2+z^2}) \times\cos(2\pi n y)-\ln\{\cosh(2\pi z) -\cos(2\pi x)\}+c_2\Bigg], \tag{7}$$

because of the x,y symmetry of the system. Equation (6) [or Eq. (7)] is rapidly convergent due to the asymptotic behavior of the modified Bessel function $K_0(x)$ as

$$K_0(x)\sim\sqrt{\frac{\pi}{2x}}\exp(-x). \tag{8}$$

In this study, we incorporate the particle-cell acceleration technique with the Lekner method in partially periodic Coulomb systems. The details of the particle-cell acceleration technique is given as follows: At first, we divide the system with size $L_{xy}\times L_{xy}\times L_z$ into $n_{xy}\times n_{xy}\times n_z$ cells. Second, the force on the ith particle $\mathbf{F}_i$ is divided into two parts as follows:

$$\mathbf{F}_i=\mathbf{F}_i^{(near)}+\mathbf{F}_i^{(far)}, \tag{9}$$

where $\mathbf{F}_i^{(near)}$ and $\mathbf{F}_i^{(far)}$ denote the force from the particles within the neighbor cells, and that from the other distant particles, respectively. In Eq. (9), $\mathbf{F}_i^{(near)}$ consists of the contribution from the particles j within the cell α given by

$$\mathbf{F}_i^{(near)} \equiv q_i \sum_{\alpha}{}' \sum_{j \in \alpha} q_j \mathbf{f}(r_{ij}), \tag{10}$$

where the first summation is taken over cells α which are sufficiently close to the particle i. In Eq. (10), $q_i q_j \mathbf{f}(r_{ij})$ is the force between the pair of particles i and j, which is given by the Lekner summation method [21]. In addition, the distant-part force $\mathbf{F}_i^{(far)}$ consists of the contribution from the particles within the cell β, which is given by

$$\mathbf{F}_i^{(far)} \equiv q_i \left\{ \sum_{\beta} Q_\beta^{(p)} \mathbf{f}(|\mathbf{r}_i - \mathbf{R}_\beta^{(p)}|) + \sum_{\beta} Q_\beta^{(m)} \mathbf{f}(|\mathbf{r}_i - \mathbf{R}_\beta^{(m)}|) \right\}, \tag{11}$$

where each summation is taken over cells β, sufficiently far from the particle i. Here $Q_\beta^{(k)}$ and $\mathbf{R}_\beta^{(k)}$ $(k=p,m)$ are cell charges and the positional vectors in the cell β, respectively. We consider particles j $(\neq i)$ in cell β with positive charges $(q_j>0)$ to evaluate the cell charges $Q_\beta^{(p)}$ and the positional vectors $\mathbf{R}_\beta^{(p)}$, and those with negative charges $(q_j<0)$ to calculate $Q_\beta^{(m)}$ and $\mathbf{R}_\beta^{(m)}$. In Eq. (11), $Q_\beta^{(k)}$ and $\mathbf{R}_\beta^{(k)}$ are defined by

$$Q_\beta^{(k)} = \sum_{j \in \beta} q_j \quad (k=p,m) \tag{12}$$

and

$$\mathbf{R}_\beta^{(k)} = \frac{\sum_{j \in \beta} q_j \mathbf{r}_j}{\sum_{j \in \beta} q_j} \quad (k=p,m). \tag{13}$$

In Eqs. (12) and (13), the summations are taken for index j with $q_j>0$ $(q_j<0)$ with respect to $k=p$ $(k=m)$. In the molecular dynamics (MD) simulations, we update the distant-part force on the ith particle $\mathbf{F}_i^{(far)}$ per n_{far} steps $(n_{far}>1)$, because $\mathbf{F}_i^{(far)}$ varies slowly compared with $\mathbf{F}_i^{(near)}$. In Eq. (9), the accuracy of the calculated force ΔF is defined to be

$$\Delta F \equiv \frac{\sum_i |\mathbf{F}_i - \tilde{\mathbf{F}}_i|^2}{\sum_i |\mathbf{F}_i|^2}, \tag{14}$$

where $\tilde{\mathbf{F}}_i$ is the force on the ith particle by direct particle-particle summations (exact values). In the following study, we obtain $\Delta F \sim 10^{-3}$ or less, which is a sufficiently accurate result. In this way, we can make the calculation of Coulomb forces in quasi-two-dimensional periodic systems much faster, and treat a lot of charged particles in the system with no difficulties.

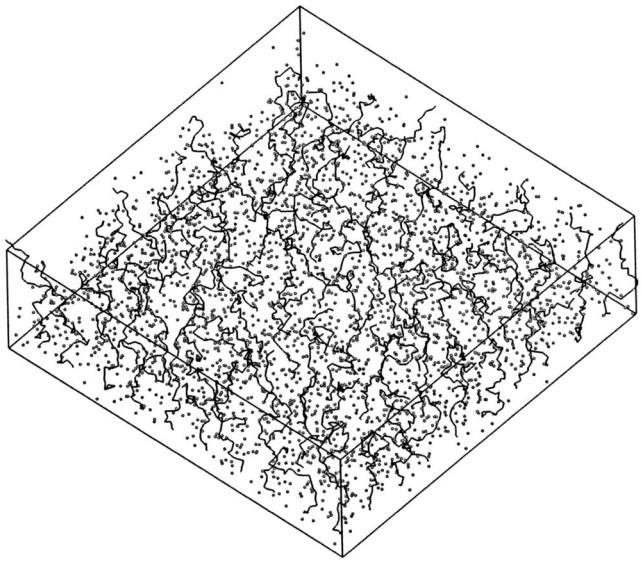

FIG. 2. Snapshot of polyelectrolyte brushes with grafting density $\rho\sigma^2=0.03$. The solid lines and filled circles denote the grafted polyelectrolyte chains and counterions, respectively.

The efficiency of the particle-cell acceleration technique is demonstrated by applying the molecular dynamics simulations on polyelectrolyte brush systems. Figure 2 is a snapshot of the polyelectrolyte brushes with the grafting density $\rho\sigma^2=0.03$. The number of polyelectrolyte chains M and the length of the chain L are taken to be $M=100$ and $L=30$, respectively, and the number of charged particles treated in this calculation is $N=6000$. In Fig. 2, solid lines and solid circles denote the grafted polyelectrolyte chains and counterions, respectively. The value of the relative dielectric constant of the medium ϵ is taken to be $\epsilon=78$, and K_{bond} in Eq. (4) is set to be $K_{bond}=30\epsilon_{LJ}/\sigma^2$.

Figure 3(a) shows the density profiles of monomers in the polyelectrolyte chains (solid line) and counterions (dashed line), respectively. The grafting density is taken to be $\rho\sigma^2=0.05$. The abscissa and the ordinate denote the rescaled distance in the z direction from the surface $z/\sigma L$, and the density distribution $n=n(z)$, respectively. The values of M and L are taken to be $M=16$ and $L=30$, and ensemble average is taken over five samples. We take 20 000 MD steps for equilibration of the system, and 100 000 MD steps for taking the statistical averages. In Fig. 3(a), we treat the salt-free system $(c_s=0.0)$, where $c_s(M)$ is the density of added salts. We can see that the thickness of the polyelectrolyte brush layers is almost $\sim 0.7\sigma L$ in this system. Figure 3(b) shows the local charge density $\rho(z)$ as a function of the distance z from the grafting surface. The profiles of the local charge density $\rho(z)$ are of great interest, because they have a great influence on various physical properties such as surface adsorption with other polyelectrolytes or charged colloids, and effective interaction between different polyelectrolyte brush layers [17]. In Fig. 3(b), the profile of $\rho(z)$ is oscillating and shows the characteristic feature at the surface of the

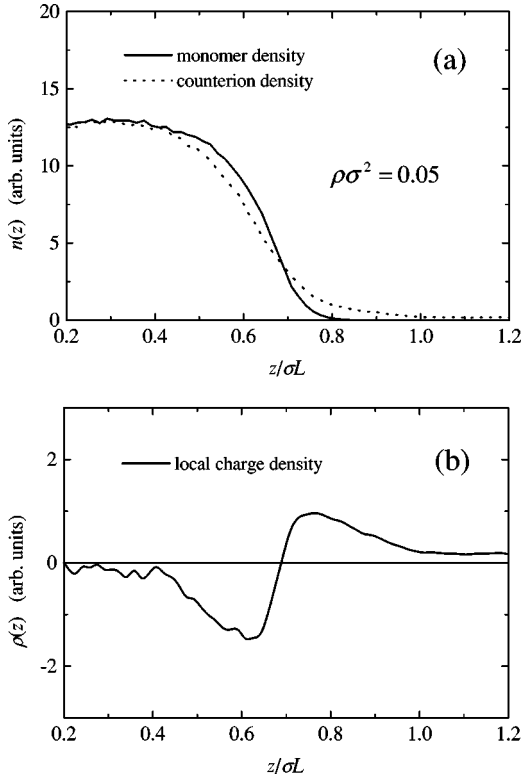

FIG. 3. (a) Density profiles of monomers (solid line) and counterions (dotted line) as a function of the distance from the grafting surface z. The grafting density is $\rho\sigma^2 = 0.05$. (b) Local charge density $\rho(z)$ as a function of the distance z.

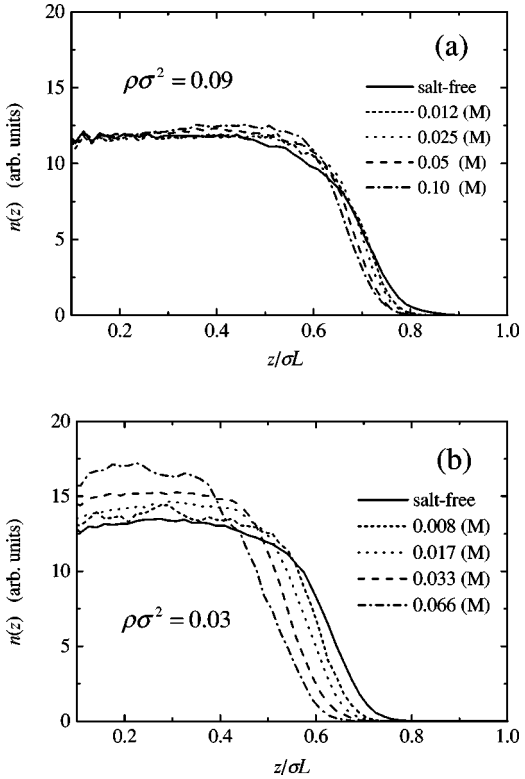

FIG. 4. (a) Density profile of monomers $n(z)$ as a function of the distance z. The grafting density is $\rho\sigma^2 = 0.09$. The added salt concentration c_s is given by $c_s = 0.0$, 0.012, 0.025, 0.05, and 0.1. (b) Density profile of monomers $n(z)$ as a function of the distance z. The grafting density is $\rho\sigma^2 = 0.03$. The added salt concentration c_s is given by $c_s = 0.0$, 0.008, 0.017, 0.033, and 0.066.

polyelectrolyte brush layers. Figure 3(b) indicates that most of the counterions are trapped inside the polyelectrolyte brush layer and other counterions diffuse outside the brush layer with thermal motions, where the global charge neutrality is satisfied.

In Figs. 4(a) and 4(b), we pay attention to the screening effect in solutions by adding 1:1 electrolyte. Figures 4(a) and 4(b) show the density profiles of monomers $n(z)$ with grafting density $\rho\sigma^2 = 0.09$ and $\rho\sigma^2 = 0.03$, respectively. In neutral polymer brush systems, the brush stretching is determined primarily by excluded-volume effects between monomers. In polyelectrolyte brushes, the brush thickness depends on electrostatic interactions with charged monomers and microions, and steric repulsion between monomers. It is anticipated that the polyelectrolyte brushes stretch by electrostatic repulsion in the brush layer, and the brushes shrink at higher salt density because of the shorter electrostatic screening length. In Fig. 4(a), the added salt concentration $c = c_s\ (M)$ is given by $c_s = 0.0$ (solid line), 0.012 (dashed line), 0.025 (dotted line), 0.05 (long-dashed line), and 0.1 (dash-dotted line). In Fig. 4(a), we can see that the density profile hardly changes with increasing the salt concentration c_s. In Fig. 4(b), the added salt concentration c_s is given by $c_s = 0.0$ (solid line), 0.008 (dashed line), 0.017 (dotted line), 0.033 (long-dashed line), and 0.066 (dash-dotted line). Figure 4(b) shows the different profiles from Fig. 4(a), where the brush thickness apparently decreases by increasing the salt concentration beyond $c_s \approx c_i$ (c_i is the counterion concentration). These results indicate that there are two distinct regimes in these systems: The excluded-volume effect is dominant at high grafting density [Fig. 4(a)], and the electrostatic screening effect becomes relevant at low grafting density [Fig. 4(b)]. These results show good agreement with recent experimental results in polyelectrolyte brushes [15].

IV. CONCLUSIONS

In conclusion, we have performed the molecular dynamics simulations of polyelectrolyte brushes in an electrolyte solution. The correct treatment of the long-range Coulomb interaction in a partially periodic system requires special methods which are computationally expensive. It is necessary to treat a lot of particles to study the screening effect by added salts, and this is a hard task in computer simulations. For this purpose, we have proposed the efficient numerical method of treating the Coulomb systems with two-dimensional periodicity. We have employed the particle-cell acceleration technique, which is incorporated with the Lekner summation method, and treated many particles with no difficulties. Using this method, we have clarified the structural formation of polyelectrolyte brushes numerically. As a result, it is found that the local charge density $\rho(z)$

shows the characteristic, oscillating feature at the surface of the brush layers. We have also studied the electrostatic screening effect on polyelectrolyte brushes by adding monovalent salts. At high grafting density, the brush height does not get influenced by added salts. At low grafting density, on the contrary, the brush height decreases with the increasing concentration of added salts. We mention that the extension of our numerical method proposed in this paper to the system with one-dimensional periodicity, i.e., solutions in nanopores, is straightforward. There are a lot of applications of this method in soft matter physics and in surface sciences (e.g., biological membranes as well as thin solid films), and these are future problems.

ACKNOWLEDGMENTS

The author would like to thank Professor T. Nakayama for valuable discussions. This work was supported in part by a Grant-in-Aid from the Japan Ministry of Education, Science, and Culture for Scientific Research. The authors thank the Supercomputer Center, Institute of Solid State Physics, University of Tokyo for the use of their facilities.

[1] *Proceedings of the Yamada Conference L*, edited by I. Noda and E. Kokufuda (Yamada Science Foundation, Osaka, 1999).
[2] J. Israelachivili, *Intermolecular and Surface Forces*, 2nd ed. (Academic Press, London, 1992).
[3] B. V. R. Tata and N. Ise, Phys. Rev. E **58**, 2237 (1998).
[4] N. Ise, T. Konishi, and B. V. R. Tata, Langmuir **15**, 4176 (1999).
[5] T. Terao and T. Nakayama, Phys. Rev. E **60**, 7157 (1999).
[6] M. Kardar and R. Golestanian, Rev. Mod. Phys. **71**, 1233 (1999), and references therein.
[7] T. Terao and T. Nakayama, J. Phys.: Condens. Matter **12**, 5169 (2000).
[8] A. Yu. Grosberg, T. T. Nguyen, and B. I. Shklovskii, Rev. Mod. Phys. **74**, 329 (2002), and references therein.
[9] T. Terao and T. Nakayama, Phys. Rev. E **63**, 041401 (2001).
[10] T. Terao and T. Nakayama, Phys. Rev. E **65**, 021405 (2002).
[11] R. W. Hockney and J. W. Eastwood, *Computer Simulation Using Particles* (IOP, Bristol, 1988).
[12] For example, Y.-J. Rhee, J. W. Halley, J. Hautman, and A. Rahman, Phys. Rev. B **40**, 36 (1989).
[13] P. Pincus, Macromolecules **24**, 2912 (1991).
[14] Y. Mir, P. Auroy, and L. Auvray, Phys. Rev. Lett. **75**, 2863 (1995).
[15] H. Ahrens, S. Förster, and C. A. Helm, Phys. Rev. Lett. **81**, 4172 (1998).
[16] E. B. Zhulina, J. K. Wolterink, and O. V. Borisov, Macromolecules **33**, 4945 (2000).
[17] Y. Tran, P. Auroy, L.-T. Lee, and M. Stamm, Phys. Rev. E **60**, 6984 (1999).
[18] S. T. Milner, Science **251**, 905 (1991).
[19] S. Alexander, J. Phys. (Paris) **38**, 983 (1977).
[20] P.-G. de Gennes, Macromolecules **21**, 1069 (1980).
[21] J. Lekner, Physica A **176**, 485 (1991).
[22] R. J. Mashl and N. Grønbech-Jensen, J. Chem. Phys. **109**, 4617 (1998).
[23] R. J. Mashl, N. Grønbech-Jensen, M. R. Fitzsimmons, M. Lütt, and D. Li, J. Chem. Phys. **110**, 2219 (1999).